Particle-number conserving analysis of the $\pi d_{5/2}$ band in ^{117,119,121,123,125}Cs*

Qing-Qing Zhang (张青青)[1] Anshul Dadwal[2] Xiao-Tao He (贺晓涛)[1†]

[1]College of Materials Science and Technology, Nanjing University of Aeronautics and Astronautics, Nanjing 210016, China
[2]Nanjing University of Aeronautics and Astronautics, Nanjing 210016, China

Abstract: The $\pi d_{5/2}$ rotational bands in odd-even nuclei ^{117,119,121,123,125}Cs are systematically investigated using the cranked shell model (CSM) with the pairing correlations modeled with a particle number conserving (PNC) method. In this PNC method, the particle number is conserved exactly while considering the blocking effects. The experimental observations of the $\pi d_{5/2}$ bands with two upbendings for ^{117,119}Cs and one backbending for ^{125}Cs are reproduced very well by the PNC-CSM method. Furthermore, $\pi d_{5/2}$ configuration bands with two upbendings for ^{121}Cs and one backbending for ^{123}Cs are predicted by the PNC-CSM calculations. The difference between the lighter ^{117,119,121}Cs and heavier ^{123,125}Cs isotopes is caused by the evolution of single-particle orbitals near the Fermi surface, and the high-j low-Ω orbital $\pi[550]1/2$ plays an important role. The proton shell gap of lighter isotopes is at $Z = 50$, whereas it appears at $Z = 48$ for heavier ones. For lighter isotopes ^{117,119,121}Cs, the first upbending is primarily due to the off-diagonal contributions of protons $j_x(\pi 5/2^-[532]\pi 3/2^-[541])$ and $j_x(\pi 1/2^-[550]\pi 3/2^-[541])$. The second upbending is mainly effected by the off-diagonal contributions of neutrons $j_x(\nu 7/2^-[523]\nu 5/2^-[532])$ and $j_x(\nu 3/2^-[541]\nu 5/2^-[532])$ for ^{117,119}Cs and $j_x(\nu 1/2^-[541]\nu 5/2^-[532])$ for ^{121}Cs, respectively. For heavier isotopes such as ^{123,125}Cs, the backbending is attributed mainly to the diagonal parts of proton $j_x(\pi 1/2^-[550])$ and neutron $\nu 7/2^-[523]$ orbital related terms of diagonal $j_x(\nu 7/2^-[523])$ and off-diagonal $j_x(\nu 7/2^-[523]\nu 5/2^-[532])$ contributions.

Keywords: cesium isotopes, particle number conserving, cranked shell model, rotational band

DOI: 10.1088/1674-1137/ae1de6 **CSTR:** 32044.14.ChinesePhysicsC.50034107

I. INTRODUCTION

The nuclei in the $A \approx 120$ mass region are generally classified as transitional and exhibit structural characteristics between spherical and well-deformed shapes ($2.0 < R_{4/2} < 3.33$). Due to their complex and diverse nuclear configurations, these nuclei are at the forefront of research on nuclear structure because they provide valuable insights into the evolution of nuclear shapes and shell structure. Recent studies on the cesium isotopic chain have revealed a variety of exotic nuclear phenomena, including shape coexistence [1], signature inversion [2], octupole correlation [3−5], band termination [6]. These phenomena have been explored through detailed experiments, including the extension of rotational bands to high spin, the measurement of isomer lifetimes, and the assignment of spin and parity for various states based on directional correlation (DCO) ratios [1, 5, 7−19]. These detailed studies have revealed unique structural properties throughout the isotopic chain.

Various theoretical models have been applied to investigate these phenomena [2, 13, 15, 16, 18, 20−26]. The characteristics of the $\pi g_{9/2}$ band in odd-A $^{119-125}$Cs nuclei are reproduced reasonably well within the framework of the particle-plus-rotor and particle-plus-vibrator models [18]. The cranked shell model (CSM) has been used to analyze the crossing frequencies for the $\pi h_{11/2}$ band and the $\pi g_{9/2}$ band in the odd-mass Cs isotopes [15]. Meanwhile, boson-fermion and core-quasiparticle coupling models have been used to describe the level structure in ^{123}Cs [13]. Although these theories explain various experimental phenomena, the upbending and backbending phenomena observed in the $\pi d_{5/2}$ band of odd-even $^{117-125}$Cs require further discussion.

Comprehensive investigations of the rotational bands in the odd-mass $^{117-125}$Cs isotopes have produced an extensive set of experimental data. These analyses have consistently revealed the occurrence of upbending and backbending phenomena in both the $\pi h_{11/2}$ and $\pi d_{5/2}$ bands across this isotopic chain. It is well known that the

Received 12 September 2025; Accepted 11 November 2025; Accepted manuscript online 12 November 2025

* This work is supported by the National Natural Science Foundation of China (12475121) and the National Key R&D Program of China (2023YFA1606503, 2024YFE0109804)

† E-mail: hext@nuaa.edu.cn

backbending and upbending phenomena are caused by the alignment of the high-j low-Ω orbitals [27]. Based on present analysis [7, 9, 12, 15, 16, 21, 28], the upbending observed in the $\pi h_{11/2}$ band at rotational frequencies around $\hbar\omega \sim 0.40$ MeV and 0.425 MeV has been attributed to the alignment of a pair of $[\nu h_{11/2}]^2$. In contrast, the $\pi d_{5/2}$ band exhibits distinct upbending and backbending at different frequencies, approximately $\hbar\omega \sim 0.20$ MeV in ^{117,119,121}Cs, and at $\hbar\omega \sim 0.40$ MeV in ^{117,119}Cs, and $\hbar\omega \sim 0.70$ MeV in ^{121}Cs, in ^{123,125}Cs the backbending exists at $\hbar\omega \sim 0.30$ MeV. The variation in the frequency for the $\pi d_{5/2}$ band across odd-mass $^{117-125}$Cs isotopes suggests that the underlying mechanism may involve contributions from different orbitals, which emphasizes the importance of further detailed investigation to elucidate the nature of these alignments.

The CSM has been applied to investigate the underlying mechanism of the upbending and backbending behavior with pairing correlations calculated using a particle-number-conserving (PNC) method to study the $\pi d_{5/2}$ band in odd-mass $^{117-125}$Cs isotopes. Unlike the conventional Bardeen-Cooper-Schrieffer (BCS) or Hartree-Fock-Bogoliubov (HFB) approaches, in the PNC-CSM method, the Hamiltonian of the ground and excited states are directly diagonalized in a large cranked many-particle configuration (CMPC) space. Thus, the particle number is conserved exactly while taking the Pauli blocking effects into account [29−31]. The PNC-CSM method has been successfully applied to describle the high-K isomers in rare-earth elements [32−36] as well as in superheavy nuclei region [37−42]. In this work, a detailed theoretical investigation of the rotational properties and pairing correlations in odd-A $^{117-125}$Cs isotopes is presented. The results provide valuable insights into the underlying nuclear structure and the evolution of configurations in these nuclei.

This paper is organized as follows. A brief introduction of the PNC treatment of pairing correlations within the CSM is presented in Sec. II. The numerical details, including the Nilsson parameters (κ, μ), deformation parameters, and pairing parameters are given in Sec. III. The PNC-CSM calculation and analysis for the $\pi d_{5/2}$ band of odd-even $^{117-125}$Cs are presented in Sec. IV. The findings are briefly summarized in Sec. V.

II. THEORETICAL FRAMEWORK

The cranked shell model Hamiltonian of an axially symmetric nucleus in the rotating frame can be written as

$$H_{\rm CSM} = H_0 + H_{\rm P} = H_{\rm Nil} - \omega J_x + H_{\rm P}, \tag{1}$$

where $H_0 = H_{\rm Nil} - \omega J_x$ is the one-body part of $H_{\rm CSM}$, $H_{\rm Nil}$ is the Nilsson Hamiltonian, $-\omega J_x$ is the Coriolis interaction with cranking frequency ω about the x axis, perpendicular to the nuclear symmetrical z axis. $H_{\rm P} = H_{\rm P}(0) + H_{\rm P}(2)$ is the pairing interaction

$$H_{\rm P}(0) = -G_0 \sum_{\xi\eta} a^\dagger_{\xi} a^\dagger_{\bar{\xi}} a_{\bar{\eta}} a_{\eta}, \tag{2}$$

$$H_{\rm P}(2) = -G_2 \sum_{\xi\eta} q_2(\xi) q_2(\eta) a^\dagger_{\xi} a^\dagger_{\bar{\xi}} a_{\bar{\eta}} a_{\eta}, \tag{3}$$

where $\bar{\xi}(\bar{\eta})$ labels the time-reversed state of a Nilsson state $\xi(\eta)$, $q_2(\xi) = \sqrt{16\pi/5}\langle\xi|r^2 Y_{20}|\xi\rangle$ is the diagonal element of the stretched quadrupole operator, and G_0 and G_2 are the effective strengths of monopole and quadrupole pairing interactions, respectively.

Instead of the usual single-particle level truncation in conventional shell model calculations, a cranked many-particle configuration truncation (Fock space truncation) is adopted. This approach is crucial to make the particle-number conserving calculations for low-lying excited states workable and sufficiently accurate. An eigenstate of $H_{\rm CSM}$ is written as

$$|\psi\rangle = \sum_i C_i |i\rangle, \tag{4}$$

where $|i\rangle$ is a CMPC (an eigenstate of the one-body operator H_0). The yrast and low-lying eigenstates can be obtained by diagonalizing $H_{\rm CSM}$ in a sufficiently large CMPC space.

The angular momentum alignment for the state $|\psi\rangle$ is

$$\langle\psi|J_x|\psi\rangle = \sum_i C_i^2 \langle i|J_x|i\rangle + 2\sum_{i<j} C_i C_j \langle i|J_x|j\rangle. \tag{5}$$

Because J_x is a one-body operator, $\langle i|J_x|j\rangle (i \neq j)$ may not vanish when two cranked many-particle configurations $|i\rangle$ and $|j\rangle$ differ by only one particle occupation [30]. After a certain permutation of creation operators, $|i\rangle$ and $|j\rangle$ can be recast into $|i\rangle = (-)^{M_{i\mu}}|\mu...\rangle$ and $|j\rangle = (-)^{M_{j\nu}}|\nu...\rangle$, where the ellipsis "..." stands for the same particle occupation and $(-1)^{M_{i\mu}} = \pm 1$, $(-1)^{M_{j\nu}} = \pm 1$ according to whether the permutation is even or odd, respectively. Therefore, the angular momentum alignment of $|\psi\rangle$ can be expressed as

$$\langle\psi|J_x|\psi\rangle = \sum_\mu j_x(\mu) + \sum_{\mu<\nu} j_x(\mu\nu), \tag{6}$$

where the diagonal contribution $j_x(\mu)$ and the off-diagonal (interference) contribution $j_x(\mu\nu)$ can be written as

$$j_x(\mu) = \langle\mu|j_x|\mu\rangle n_\mu, \tag{7}$$

$$j_x(\mu\nu) = 2\langle\mu|j_x|\nu\rangle\sum_{i<j}(-1)^{M_{i\mu}+M_{j\nu}}C_iC_j, \quad (\mu \neq \nu), \tag{8}$$

where $n_\mu = \sum_i |C_i|^2 P_{i\mu}$, is the occupation probability of the cranked orbital $|\mu\rangle$, $P_{i\mu} = 1$ if $|\mu\rangle$ is occupied in $|i\rangle$, and $P_{i\mu} = 0$ otherwise.

III. NUMERICAL DETAILS

In the present study, the Nilsson parameters κ and μ for the odd-mass $^{117-125}$Cs are adopted from Ref. [43]. The effective pairing strengths can be determined based on the odd-even mass differences in binding energies and are closely related to the size of the truncated CMPC space. For the odd-even $^{117-125}$Cs isotopes, the CMPC space is constructed for both protons and neutrons using the major shells from $N = 3$ to $N = 5$, with the dimension of the configuration space set to a value of approximately 1000 for both protons and neutrons. The corresponding effective pairing strengths used in the calculations for ^{117,119,121}Cs are $G_{0p} = 0.52$ MeV, $G_{2p} = 0.003$ MeV, $G_{0n} = 0.70$ MeV and $G_{2n} = 0$ MeV. For ^{123,125}Cs, the effective pairing strengths are $G_{0p} = 0.48$ MeV, $G_{2p} = 0.01$ MeV, $G_{0n} = 0.70$ MeV and $G_{2n} = 0.03$ MeV.

The deformation parameters $(\varepsilon_2, \varepsilon_4)$ adopted in the present study for the odd-mass $^{117-125}$Cs isotopes are listed in Table 1. Among these nuclei, an experimental value of the quadrupole deformation parameter $\varepsilon_2 = 0.32$, has been reported only for the $\pi g_{9/2}$ band in ^{119}Cs [44]. The rotational band structures of ^{117}Cs and ^{121}Cs exhibit similar characteristics to those observed in ^{119}Cs. Hence, their deformation parameters are adopted based on the analysis of ^{119}Cs. Meanwhile, the rotational behaviors of ^{123}Cs and ^{125}Cs resemble those of ^{113}Cs [45], and their deformation parameters are taken from Ref. [46]. It may be observed that the ε_2 adopted in the present study decreases with the number of neutrons increasing, which is consistent with prior results [18, 46].

Figure 1 presents the calculated band-head energies of the $\pi g_{9/2}$ band obtained using the PNC-CSM approach. The theoretical results are in good agreement with the experimental data, which supports the reliability of the deformation parameters adopted for the odd-even $^{117-125}$Cs isotopes.

IV. RESULTS AND DISCUSSIONS

Figure 2 shows the calculated cranked Nilsson levels near the Fermi surface of ^{121}Cs and ^{125}Cs. The positive (negative) parity levels are denoted by blue (red) lines. The signature $\alpha = +1/2$ ($\alpha = -1/2$) levels are denoted by solid (dotted) lines. The cranked Nilsson level structures near the Fermi surface of ^{117}Cs and ^{119}Cs are similar to those of ^{121}Cs, while the levels near the Fermi surface of ^{123}Cs exhibit similarities to those of ^{125}Cs. These diagrams were employed to determine the quasiparticle orbitals in closest proximity to the proton and neutron Fermi surfaces [9]. Note that, for ^{121}Cs, the $\pi[420]1/2$, $\pi[422]3/2$, $\pi[550]1/2$, and $\pi[541]3/2$ ortitals are close to each other, and the components of the bands built on those orbitals may therefore mix. In the present calculation, it is evident that there is a neutron gap at $N = 60$ and proton gaps at $Z = 50$ and 60 in ^{121}Cs. With decreasing ε_2, the $\pi[431]1/2$ orbital approaches the Fermi surface, resulting in a shift of the proton shell gap from $Z = 50$ to $Z = 48$. For neutrons, a subshell gap is observed at $N = 70$ for ^{125}Cs.

Figure 3 shows the experimental and calculated MOIs and alignments of the $\pi d_{5/2}$ band in odd-even $^{117-125}$Cs. The experimental MOIs and alignments are denoted by solid dots (α=+1/2). The calculated MOIs and alignments are denoted by solid (α=+1/2) and dashed lines (α=–1/2). The PNC-CSM calculations identify this band as the $\pi 1/2^+[420]$ configuration, an orbital that originates from the $\pi d_{5/2}$ spherical shell. Only the theoretical results are displayed because no experimental data are available for $\alpha = -1/2$. The PNC-CSM calculations agree well with the experimental data for ^{117}Cs and ^{119}Cs. For ^{121}Cs, where experimental data are unavailable, only calculated results are presented. For ^{123}Cs and ^{125}Cs, the calculated results show satisfactory agreement with the experimental data, exhibiting only small discrepancies. As shown in Fig. 3, the first upbending in ^{117,119}Cs occurs at a rotational frequency of approximately $\hbar\omega \sim 0.20$ MeV, followed

Table 1. Deformation parameters $(\varepsilon_2, \varepsilon_4)$ used in the PNC-CSM calculations for odd-even $^{117-125}$Cs.

	^{117}Cs	^{119}Cs	^{121}Cs	^{123}Cs	^{125}Cs
ε_2	0.330	0.320	0.315	0.228	0.223
ε_4	0.020	0.010	0.018	0.032	0.030

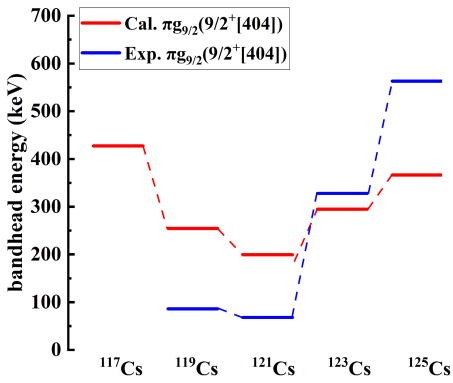

Fig. 1. (color online) Experimental and calculated band-head energies of the $\pi g_{9/2}$ band built on the $\pi[404]9/2^+$ orbital in odd-even $^{117-125}$Cs. The experimental band-head energies are denoted by blue lines. The calculated band-head energies are denoted by red lines.The experimental data were sourced from prior works [9, 10, 12, 47].

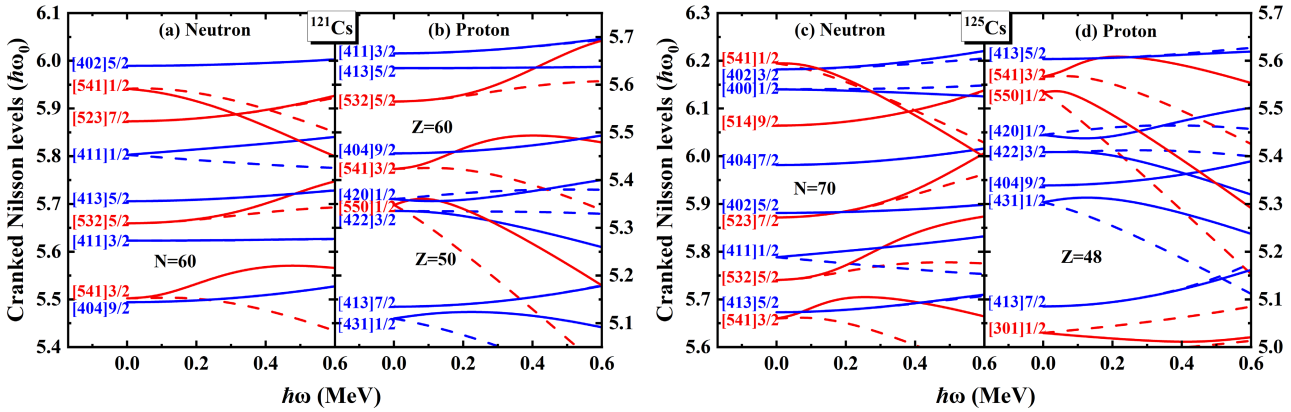

Fig. 2. (color online) Single-particle Routhians located in the vicinity of the Fermi level of ^{121}Cs and ^{125}Cs as a function of rotational frequency for (a) and (b) cranked Nilsson levels of ^{121}Cs and (c) and (d) cranked Nilsson levels of ^{125}Cs. Positive (negative) parity Routhians are shown by blue (red) lines. Solid (dotted) lines show the signature $\alpha = +1/2$ ($\alpha = -1/2$).

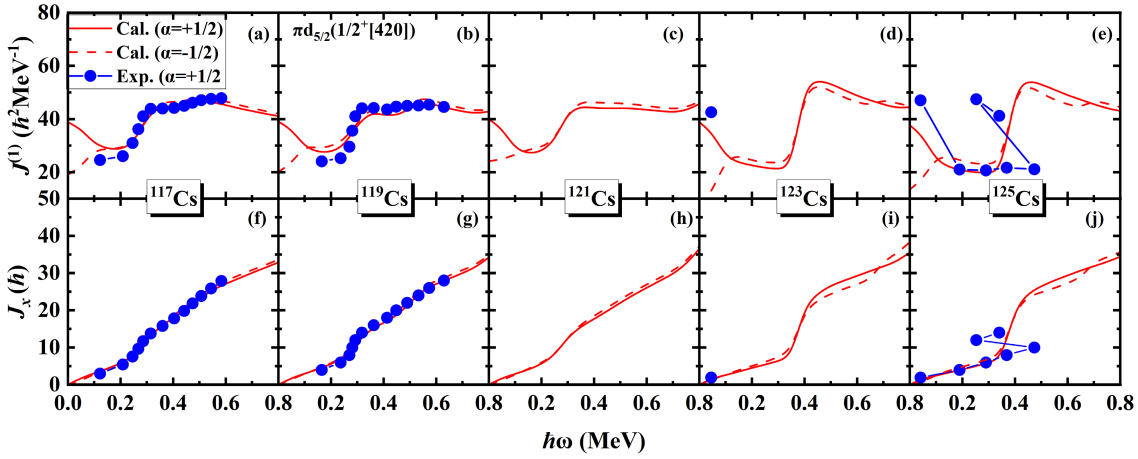

Fig. 3. (color online) Experimental and calculated MOIs $J^{(1)}$ (upper panels) and alignments J_x (lower panels) of the $\pi d_{5/2}(1/2^+[420])$ band in odd-even $^{117-125}$Cs. The experimental MOIs and alignments are denoted by solid dots (α=+1/2). The calculated MOIs and alignments are denoted by solid lines (α=+1/2) and dashed lines (α=—1/2). The experimental data were obtained from prior works [7, 9, 10, 12].

by a second upbending around $\hbar\omega \sim 0.40$ MeV. In the case of ^{121}Cs, the first upbending is similar to that in ^{117,119}Cs, which is observed near $\hbar\omega \sim 0.20$ MeV. The cranked Nilsson levels for ^{121}Cs are similar to those for ^{117}Cs and ^{119}Cs, but the neutron Fermi surface changes with the increase in neutron number. Therefore, the second upbending for ^{121}Cs shifts to a higher frequency around $\hbar\omega \sim 0.70$ MeV. For the heavier isotopes ^{123}Cs and ^{125}Cs, the backbending occurs around $\hbar\omega \sim 0.30$ MeV. These systematic variations indicate that the rotational behavior of the $\pi d_{5/2}(1/2^+[420])$ band evolves with an increasing mass number in the odd-mass Cs isotopes. It is well known that backbending phenomena is associated with the alignment of high-j intruder orbitals [27], which correspond to the proton and neutron $h_{11/2}$ orbitals in this mass region [46]. The different upbending and backbending mechanisms in odd-even $^{117-125}$Cs are discussed separately in the following.

In the PNC method, the total particle number $N = \sum_\mu n_\mu$ is exactly conserved, whereas the probability of occupation n_μ for each orbital varies with rotational frequency $\hbar\omega$. This is a key advantage of the PNC approach, as it allows for a more detailed investigation of the evolution of Nilsson levels with rotation. By analyzing the ω dependence of orbitals near to the Fermi surface, valuable insights into the upbending and backbending mechanism can be obtained. The occupation probability n_μ of each orbital μ near the Fermi surface of the $\pi d_{5/2}(1/2^+[420])$ band in ^{117,119,121}Cs are shown in Fig. 4. The top and bottom rows show data for protons and neutrons, respectively. The positive (negative) parity is denoted by blue solid lines (red dotted lines). It is evident from Fig. 4 that, around the rotational frequency $\hbar\omega \sim 0.20$ MeV for ^{117,119,121}Cs, the occupation probability of $\pi[550]1/2$ ($\pi h_{11/2}$) increases sharply from 1.5 to nearly 2.0, whereas the occupation probabilities of

π[541]3/2 and π[532]5/2 decrease. This behavior can be understood from Fig. 2. With increasing $\hbar\omega$, the π[541]3/2 and π[532]5/2 orbitals gradually move away from the Fermi surface, whereas the π[550]1/2 orbital approaches it. As a result, the occupation probabilities of the π[541]3/2 and π[532]5/2 orbitals decrease with increasing cranking frequency, whereas the occupation probability of the π[550]1/2 orbital increases. For the second upbending of ^{117,119,121}Cs, Fig. 4(d) shows the occupation probabilities of ν[541]3/2 and ν[411]3/2 increase around $\hbar\omega \sim 0.40$ MeV, while the occupation probability ν[532]5/2 sharply decreases. In Fig. 4(e), around the upbending frequency, the occupation probability of ν[541]3/2 and ν[532]5/2 increase correspondingly while other the occupation probabilities orbitals decrease. For ^{121}Cs, around $\hbar\omega \sim 0.70$ MeV, the occupation probability ν[532]5/2 sharply increases, while the occupation probability ν[541]1/2 decreases. Similarly, the occupation probability n_μ of each orbital μ near the Fermi surface of the $\pi d_{5/2}(1/2^+[420])$ band in ^{123,125}Cs are shown in Fig. 5. In Fig. 5, the occupation probability of π[550]1/2 increases gradually from nearly 0 to 2 around $\hbar\omega \sim 0.30$ MeV, while the occpution of π[422]3/2,π[404]9/2, and π[420]1/2 decrease. For neutrons, the occupation probability of ν[523]7/2 approaches 0 at $\hbar\omega \sim$ 0.30 MeV, while the occupation probabilities of other orbitals become larger. It may be observed that the first upbending of ^{117,119,121}Cs primarily comes from the contributions of the $\pi h_{11/2}$ orbitals and the second upbending of ^{117,119,121}Cs mainly comes from the contributions of the $\nu h_{11/2}$ orbitals. For ^{123,125}Cs, the observed backbending arises predominantly from the combined contributions of both the $\pi h_{11/2}$ and $\nu h_{11/2}$ orbitals.

In order to understand clearly the mechanism of upbending and backbending, the contributions of each proton and neutron major shell to the angular momentum alignment $\langle J_x \rangle$ for the $\pi d_{5/2}(1/2^+[420])$ band in odd-even $^{117-125}$Cs are shown in Fig. 6 and Fig. 7. The contributions of diagonal $\sum_\mu j_x(\mu)$ and off-diagonal $\sum_{\mu<\nu} j_x(\mu\nu)$ from the neutron $N = 5$ and proton $N = 5$ major shells are shown as dashed lines. The first upbending observed in the $\pi d_{5/2}(1/2^+[420])$ band of ^{117,119,121}Cs around $\hbar\omega \sim$ 0.20 MeV is primarily attributed to the contribution of the proton $N = 5$ shell. Furthermore, it mainly originates from the off-diagonal part of the proton $N = 5$ shell, whereas the diagonal part provides a relatively smaller contribution to upbending. For the second upbending observed in ^{117,119,121}Cs, there is no significant contribution from the proton $N = 4,5$ shells, the upbending is predominantly driven by the contribution of neutron $N = 5$ shell. For ^{117}Cs, the dominant contribution arises from the off-diagonal part of the neutron $N = 5$ shell, whereas the diagonal part contributes only marginally. Similarly, in ^{119,121}Cs, the second upbending is mainly driven by the off-diagonal part of the neutron $N = 5$ shell. Fig. 7 shows

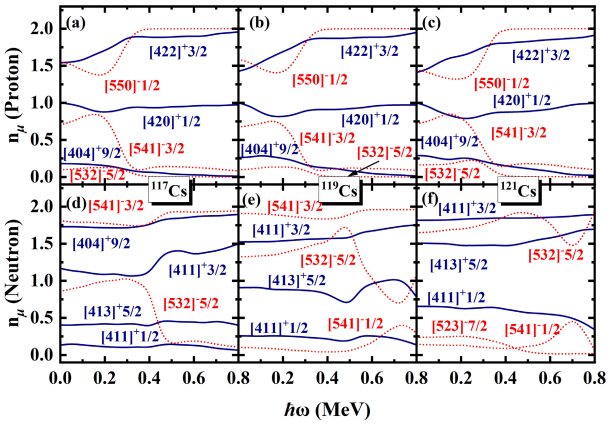

Fig. 4. (color online) Occupation probability n_μ of each orbital μ near the Fermi surface for the $\pi d_{5/2}(1/2^+[420])$ band in ^{117,119,121}Cs. The top and bottom rows show protons ($\alpha = +1/2$) and neutrons, respectively. The positive (negative) parity is denoted by blue solid lines (red dotted lines). The Nilsson levels far above the Fermi surface ($n_\mu \sim 0$) and far below ($n_\mu \sim 2$) are not shown.

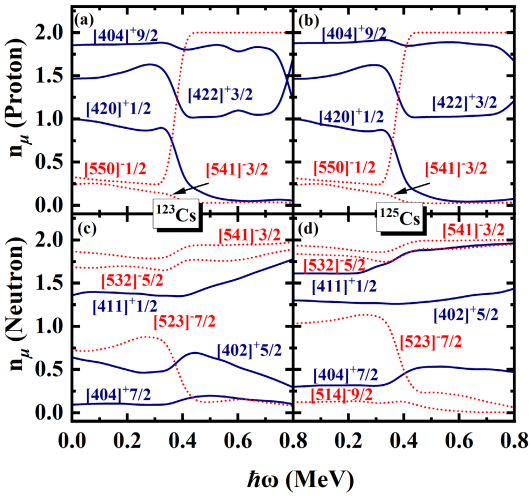

Fig. 5. (color online) The same as in Fig. 4 but for ^{123,125}Cs.

that the angular momentum alignments increase with 12.5$\hbar$ and 20$\hbar$ at $\hbar\omega \sim 0.30$ MeV for neutron and proton $N = 5$ shells, respectively. This simultaneous alignment leads to the backbending observed in the $\pi d_{5/2}(1/2^+[420])$ band of ^{123,125}Cs. The backbending is primarily driven by both the diagonal and off-diagonal components of the neutron $N = 5$ shell, along with the diagonal part of the proton $N = 5$ shell. In contrast, the off-diagonal part of the proton $N = 5$ shell contributes relatively little to the backbending.

For a deep insight into the upbending and backbending mechanism, the contribution of each proton orbital and neutron orbital in the $N = 5$ major shell to the angular momentum alignments $\langle J_x \rangle$ for the $\pi d_{5/2}(1/2^+[420])$ band in odd-even $^{117-125}$Cs are presented in Fig. 8 and Fig. 9. The diagonal (off-diagonal) part $j_x(\mu)$ ($j_x(\mu\nu)$) is

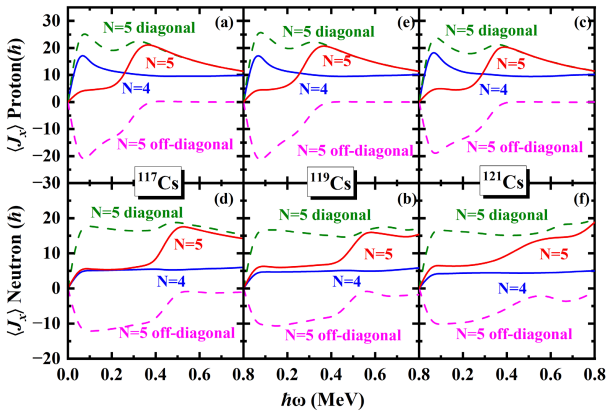

Fig. 6. (color online) Contribution of each proton and neutron major shell to the angular momentum alignment $\langle J_x \rangle$ for the $\pi d_{5/2}(1/2^+[420])$ band in ^{117,119,121}Cs. The contributions of diagonal $\sum_\mu j_x(\mu)$ and off-diagonal $\sum_{\mu<\nu} j_x(\mu\nu)$ from the neutron $N=5$ and proton $N=5$ major shells ($\alpha=+1/2$) are shown as dashed lines.

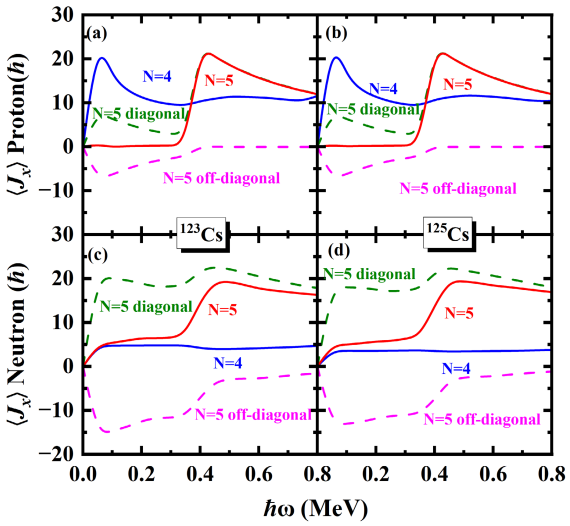

Fig. 7. (color online) As in Fig. 6 but for ^{123,125}Cs.

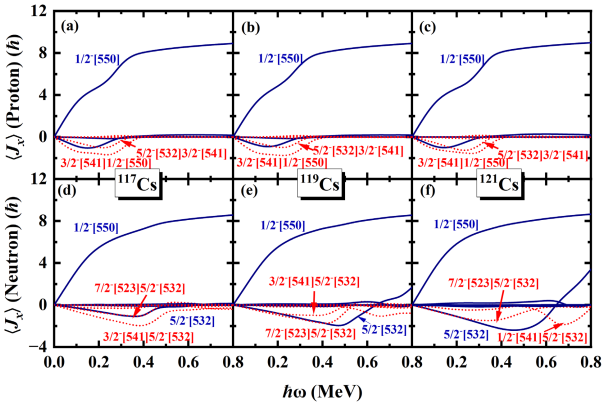

Fig. 8. (color online) Contribution of each proton orbital for $\alpha=+1/2$ (top) and neutron orbital (bottom) in the $N=5$ major shell to the angular momentum alignments $\langle J_x \rangle$ for the $\pi d_{5/2}(1/2^+[420])$ band in odd-even ^{117,119,121}Cs. The diagonal (off-diagonal) part $j_x(\mu)[(j_x(\mu\nu)]$ is denoted by blue solid (red dotted) lines.

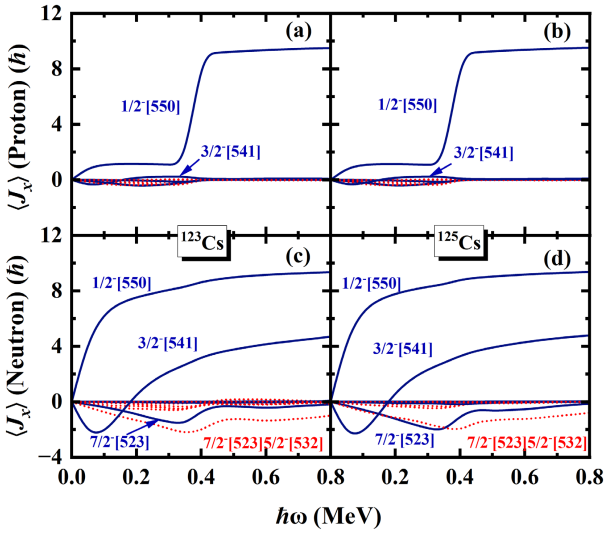

Fig. 9. (color online) As in Fig. 8 but for ^{123,125}Cs.

denoted by blue solid lines (red dotted). In Fig. 8 (a)–(c), around $\hbar\omega \sim 0.20$ MeV, it is evident that the off-diagonal contributions $j_x(\pi 5/2^-[532]\pi 3/2^-[541])$ and $j_x(\pi 1/2^-[550]\pi 3/2^-[541])$ increase significantly with increasing rotational frequency in ^{117,119,121}Cs. These off-diagonal matrix elements are responsible for the first upbending observed in these nuclei. In Fig. 8(d), it may be observed that the diagonal part $j_x(\nu 5/2^-[532])$ and the off-diagonal parts $j_x(\nu 7/2^-[523]\nu 5/2^-[532])$ and $j_x(\nu 3/2^-[541]\nu 5/2^-[532])$ contribute to the second upbending of ^{117}Cs. In Fig. 8(e), the second upbending of ^{119}Cs is attributed to the off-diagonal parts $j_x(\nu 7/2^-[523]\nu 5/2^-[532])$ and $j_x(\nu 3/2^-[541]\nu 5/2^-[532])$. In ^{121}Cs, the second upbending is mainly driven by the off-diagonal part $j_x(\nu 1/2^-[541]\nu 5/2^-[532])$. For ^{123,125}Cs, the diagonal part $j_x(\pi 1/2^-[550])$ increases from $2\hbar$ at $\hbar\omega \sim 0.30$ MeV to $9\hbar$ at $\hbar\omega \sim 0.40$ MeV. It provides the main contributions to the backbending of $\pi d_{5/2}(1/2^+[420])$ band in ^{123,125}Cs. Moreover, the backbending is effected by the neutron with the off-diagonal part $j_x(\nu 5/2^-[532]\nu 7/2^-[523])$ and diagonal part $j_x(\nu 7/2^-[523])$ increasing slightly at $\hbar\omega \sim 0.30$ MeV.

V. SUMMARY

In this study, the $\pi d_{5/2}$ bands for odd-even $^{117-125}$Cs are investigated using the PNC-CSM. The calculated band-head energies of the $\pi g_{9/2}$ band show good agreement with experimental data. The experimental moments of inertia and alignments are reproduced well by the PNC calculations. A comprehensive understanding of the upbending and backbending phenomena in each nucleus is

achieved by analyzing the ω dependence of the occupation probability of each cranked Nilsson orbital near the Fermi surface, as well as the contributions of valence orbitals to the angular momentum alignment within each major shell. The first upbending in the $\pi d_{5/2}$ band of ^{117,119,121}Cs is primarily caused by the off-diagonal contribution of $j_x(\pi 5/2^-[532]\pi 3/2^-[541])$ and $j_x(\pi 1/2^-[550]\pi 3/2^-[541])$, whereas the second upbending is driven by the off-diagonal parts of the $j_x(\nu 7/2^-[523]\nu 5/2^-[532])$ and $j_x(\nu 3/2^-[541]\nu 5/2^-[532])$ for ^{117,119}Cs and the $j_x(\nu 1/2^-[541]\nu 5/2^-[532])$ for ^{121}Cs. In contrast, for ^{123,125}Cs, the backbending of the $\pi d_{5/2}$ band arises from the combined contributions of the diagonal $j_x(\pi 1/2^-[550])$ and $j_x(\nu 7/2^-[523])$ and the off-diagonal $j_x(\nu 7/2^-[523]\nu 5/2^-[532])$. These differences in rotational behavior between ^{117,119,121}Cs and ^{123,125}Cs can be attributed to the evolution of single-particle orbitals near the Fermi surface. With increasing neutron number, the $\pi[550]1/2$ orbital moves away from the Fermi surface, which leads to a shift in the crossing frequencies. Consequently, the single-particle evolution drives the proton shell gap from $Z = 50$ to $Z = 48$.

References

[1] K. K. Zheng, C. M. Petrache, Z. H. Zhang *et al.*, Phys. Lett. B **822**, 136645 (2021)
[2] Y. Z. Liu, J. B. Lu, Y. J. Ma *et al.*, Phys. Rev. C **54**, 719 (1996)
[3] B. F. Lv, C. M. Petrache, K. K. Zheng *et al.*, Phys. Rev. C **105**, 044319 (2022)
[4] J. F. Smith, C. J. Chiara, D. B. Fossan *et al.*, Phys. Rev. C **57**, R1037 (1998)
[5] K. Selvakumar, A. K. Singh, C. Ghosh *et al.*, Phys. Rev. C **92**, 064307 (2015)
[6] R. Wadsworth, E. S. Paul, A. Astier *et al.*, Phys. Rev. C **62**, 034315 (2000)
[7] P. M. Jodidar, C. M. Petrache, X. T. He *et al.*, Phys. Rev. C **110**, 044304 (2024)
[8] K. K. Zheng, C. M. Petrache, Z. H. Zhang *et al.*, Eur. Phys. J. A **58**, 50 (2022)
[9] K. K. Zheng, C. M. Petrache, Z. H. Zhang *et al.*, Phys. Rev. C **104**, 044305 (2021)
[10] J. Sun, Y. J. Ma, T. Komatsubara *et al.*, Phys. Rev. C **93**, 064301 (2016)
[11] K. Singh, S. Sihotra, S. S. Malik *et al.*, Eur. Phys. J. A **27**, 321 (2006)
[12] K. Singh, Z. Naik, R. Kumar *et al.*, Eur. Phys. J. A **25**, 345 (2005)
[13] A. Gizon, B. Weiss, P. Paris *et al.*, Eur. Phys. J. A **8**, 41 (2000)
[14] M. Sugawara, H. Kusakari, T. Murakami *et al.*, Eur. Phys. J. A **2**, 237 (1998)
[15] J. R. Hughes, D. B. Fossan, D. R. LaFosse *et al.*, Phys. Rev. C **45**, 2177 (1992)
[16] J. R. Hughes, D. B. Fossan, D. R. LaFosse *et al.*, Phys. Rev. C **44**, 2390 (1991)
[17] P. Chowdhury, U. Garg, T. P. Sjoreen *et al.*, Phys. Rev. C **23**, 733 (1981)
[18] U. Garg, T. P. Sjoreen, and D. B. Fossan, Phys. Rev. C **19**, 217 (1979)
[19] C. Droste, T. Morek, S. G. Rohozinski *et al.*, J. Phys. G: Nucl. Part. Phys. **18**, 1763 (1992)
[20] X. Zheng, W. P. Zeng, X. Q. Chen *et al.*, Chin. Phys. C **20**, 639 (1996)
[21] J. F. Smith, V. Medina-Chico, C. J. Chiara *et al.*, Phys. Rev. C **63**, 024319 (2001)
[22] K. Selvakumar, A. K. Singh, S. Das *et al.*, Phys. Rev. C **88**, 024313 (2013)
[23] G. Bhat, R. Ali, J. Sheikh *et al.*, Nucl. Phys. A **922**, 150 (2014)
[24] S. Y. Wang, B. Qi, and D. P. Sun, Phys. Rev. C **82**, 027303 (2010)
[25] G. Bhat, J. Sheikh, and R. Palit, Phys. Lett. B **707**, 250 (2012)
[26] E. Mardones, J. Barea, C. E. Alonso *et al.*, Phys. Rev. C **93**, 034332 (2016)
[27] F. S. Stephens, Rev. Mod. Phys. **47**, 43 (1975)
[28] X. Sun, Z. Liu, X. Zhou *et al.*, Phys. Rev. C **51**, 2803 (1995)
[29] C. S. Wu and J. Y. Zeng, Phys. Rev. C **39**, 666 (1989)
[30] J. Y. Zeng, T. H. Jin, and Z. J. Zhao, Phys. Rev. C **50**, 1388 (1994)
[31] X. B. Xin, S. X. Liu, Y. A. Lei *et al.*, Phys. Rev. C **62**, 067303 (2000)
[32] Z. H. Zhang, M. Huang, and A. V. Afanasjev, Phys. Rev. C **101**, 054303 (2020)
[33] X. T. He and Y. C. Li, Phys. Rev. C **98**, 064314 (2018)
[34] Z. H. Zhang, Y. A. Lei, and J. Y. Zeng, Phys. Rev. C **80**, 034313 (2009)
[35] B. H. Li, Z. H. Zhang, and Y. A. Lei, Chin. Phys. C **37**, 014101 (2013)
[36] X. T. He, Y. Cao, and X. L. Gan, Phys. Rev. C **102**, 014322 (2020)
[37] Z. H. Zhang, X. T. He, J. Y. Zeng *et al.*, Phys. Rev. C **85**, 014324 (2012)
[38] Y. C. Li and X. T. He, Science China Physics, Mechanics & Astronomy **59**, 672011 (2016)
[39] X. T. He, S. Y. Zhao, Z. H. Zhang *et al.*, Chin. Phys. C **44**, 034106 (2020)
[40] X. T. He, Z. Z. Ren, S. X. Liu *et al.*, Nucl. Phys. A **817**, 45 (2009)
[41] Z. H. Zhang, J. Y. Zeng, E. G. Zhao *et al.*, Phys. Rev. C **83**, 011304 (2011)
[42] Z. H. Zhang, J. Meng, E. G. Zhao *et al.*, Phys. Rev. C **87**, 054308 (2013)
[43] T. Bengtsson and I. Ragnarsson, Nucl. Phys. A **436**, 14 (1985)
[44] C. Thibault, F. Touchard, S. Büttgenbach *et al.*, Nucl. Phys. A **367**, 1 (1981)
[45] Z. H. Zhang and P. Xu, Chin. Phys. C **41**, 024103 (2017)
[46] P. Moller, J. Nix, W. Myers *et al.*, Atomic Data Nucl. Data Tables **59**, 185 (1995)
[47] J. Genevey, A. Gizon, G. Marguier *et al.* (The Isolde and Isolde Collaboration), Z. Phys. A **338**, 405 (1991)